PROBING THE Z=6 SHELL GAP IN ^{18}C: Study of the Spin-Orbit $1p_{1/2}$ -$1p_{3/2}$ splitting

Magic numbers arising from large energy gaps between shells are the corner stones of nuclear structure. These numbers, as described by Goepper-Mayer and Jensen in their pioneer work [Goe49], can be divided in two types, those due to the harmonic oscillator potential (HO), (2, 8, 20), and those originated from the spin-orbit (SO) coupling between the spin of the nucleon and its orbital motion (28, 50, 82,126). In nuclear physics, the spin-orbit splitting of the single-particle states plays a very important role. Its origin has been studied in the past, but it is still far from being well understood [Pie93]. Theoretically, a detail knowledge of the origin of the spin-orbit coupling remains unknown owing to the difficulty to describe the structure of nuclei from ab-initio theories using two (2N) and three nucleon forces (3NF). Experimentally, important efforts to study the spin-orbit splitting at N=28 and the properties of the two-body spin-orbit interaction have been made with great success [Gau06,Bur14]

From all the magic numbers that emerge as a consequence of the spin-orbit splitting, the gaps at 6 and 14, were already considered by Goepper-Mayer and Jensen as very weak [Goe63]. However, experimental results of the energy of the first 2^+ state at 7.012 MeV in ^{14}C [Ajz91] combined with systematics of the proton distribution radii of N=8 isotones point out to the possible existence of a Z=6 shell closure. In addition, the small B(E2) values obtained from lifetime measurements of the first 2^+ states in other neutron-rich carbon isotopes $^{16\text{-}18}$C [Ima04,Wie08,Ong08,Pet12,Vos12] do also suggest the appearance of a new proton magic number at Z=6 in this region. Just recently a compilation of results published in Nature [Ong18] based on a systematic analysis of the point-proton distribution radii, electromagnetic transitions B(E2), and atomic masses of light nuclei showed evidence for a Z=6 shell closure in $^{13\text{-}20}$C isotopes.

However, taking as a starting point ^{14}C, a reduction of the spin-orbit splitting could also be expected owing to a modified proton-neutron interaction as we fill in the neutron $d_{5/2}$ orbital [Ots05]. In ^{14}C, five strong l=1 transitions have been observed at 0, 7.01, 8.32 10.45 and 11.35 MeV. The ground state contains the $1p_{1/2}$ and the other four separated by approximately 7 MeV will correspond to the spin-orbit partner $1p_{3/2}$, but no measurement of the Z=6 gap is available after ^{14}C. A widening or reduction of the gap between the $1p_{1/2}$ and $1p_{3/2}$ orbitals as we add neutrons to the $1d_{5/2}$ should have crucial implications in the structure of neutron-rich carbon isotopes and it is important to study. In order to firmly stablish the emergence of a new proton magic number at Z=6, proton single-particle states in neutron-rich carbon isotopes have to be measured. Therefore, we propose to study the spin-orbit $1p_{1/2}$-$1p_{3/2}$ splitting using the d(^{19}N,^{3}He)^{18}C reaction which will selectively populate the proton single-particle states in ^{18}C. So far, the knowledge on the spectroscopy of ^{18}C is limited to in-beam γ-ray spectroscopy [Sta08], lifetime measurements [Ong08, Vos12], and one-neutron removal from ^{19}C [Kond09]. Just recently an experiment from the R^{3}B collaboration performed at GSI using the ^{19}N(p,2p)^{18}C analogue reaction of (d,^{3}He), which focused on the study of core+4n correlations [Ald18], showed two structures above the S_n=4.18 MeV, and another one above the S_{2n}=4.92 MeV [AldT18]. However, only the first one showed the characteristic l=1 value of a 1p-hole state. Besides, the structures are rather wide, owing partially to the resolution of the neutron detection, and it is difficult to know whether there should be more resonances or if the resonances are just broad.

The use of the (d,^{3}He) transfer reaction represents some assets with respect to the previous knockout (p,2p) experiment since we will be able to determine the excitation energy spectrum and to extract the angular distribution information with unprecedented resolution. This allows to determine unambiguously spin and parities of the states populated in the reaction, including bound and unbound states. Finally, absolute determination of the excitation energy and not relative energy is possible.

The present study provides a unique way of determining the gap between the $1p_{1/2}$ and $1p_{3/2}$ single-particle states and will help to constraint the microscopic origin of the spin-orbit splitting. In the case of ^{18}C, the proximity to the continuum, the proton-neutron asymmetry of the fermi surfaces for protons and neutrons, would be an interesting testing ground for ab-initio structure calculations.

In addition, in this experiment we will measure simultaneously neutron-removal states in ^{18}N via the (d,t) reaction. The main interest here focuses on the study of cross-shell states, those with positive parity in ^{18}N which are difficult to describe by shell model calculations. It is known that the excitation energies of the first 2^+ states in ^{16}C, ^{18}C and ^{20}C [Sta08] observed at 1.766(10), 1.585(10) and 1.588(20) MeV are overpredicted by 600 keV by shell model calculations using the WBT interaction within the *spsdpf* space allowing 0hw excitations. In order to fix this disagreement a reduction of the neutron-neutron nuclear matrix element, which was element dependent, had to be included ad-hoc WBT*. Surprisingly, this reduction was not enough to properly account for the positions of high-lying positive parity states in ^{17}C, as recently measured in an neutron removal experiment from ^{18}C at RIKEN [Kim18], and had serious difficulties to predict the excitation energies of the cross-shell states that have negative parity in ^{17}C. However, the recently developed YSOX interaction which includes the monopole-based universal interaction V_{MU} for the cross-shell two-body matrix elements and allows larger hw excitations successfully reproduced the ^{17}C spectrum including cross-shell states.

Since the single-particle energies of the cross-shell states are a measurement of the shell gap at N=8, identifying such states and their spectroscopic strength along the N=11 isotonic chain ^{16}B,^{17}C and ^{18}N will provide a measurement of how the shell gap evolves with Z. In ^{18}N using a simple Independent Particle Model, the protons occupy the $\pi p_{1/2}$ orbital and the neutrons are mainly located in the $\nu d_{5/2}$ orbital. Cross-shell states will be populated when removing neutrons from the $\nu p_{1/2}$ orbital.

The levels anticipated to be populated in the d(^{19}N,^{3}He)^{18}C and d(^{19}N,^{3}H)^{18}N reaction have been estimated from shell model calculations using the code Oxbash and the WBT* interaction [Sta08] (see Table 1). In the case of the d(^{19}N,^{3}He)^{18}C, it is worth noticing that the states of interest are at high excitation energies and have not been observed so far, apart maybe from the first one at 6.43 MeV, that corresponds to a l=1 resonance at 5.6 MeV in the work of [Ald18]. Removing a proton from the $1p_{1/2}$ orbital will populate the ground 0^+ state in ^{18}C. The anticipated spectroscopic factor to this state shows that the full strength of the $1p_{1/2}$ orbital is exhausted with the ground 0^+ state. Now, the position of the proton single-particle $1p_{3/2}$ energy is not known. Shell model calculations predict a couple of strong 2^+ states in ^{18}C at 6.43 and 8.09 MeV (S_n=4.18 MeV) and two significant 1^+ states at approximately 10 MeV of excitation energy that carry a significant strength of the $1p_{3/2}$ orbital. Those states will be observed in our experiment and the measurement of the spectroscopic factors will provide a testing ground for the Z=6 shell gap. It should be noticed, that most of the states are placed above the one and two neutron-separation threshold (S_n=4.18 MeV) and (S_{2n}=4.92 MeV). The single-particle widths are expected to become wider as the excitation energy increases.

In the case of the d(^{19}N,^{3}H)^{18}N reaction, cross-shell states with significant strength are expected to appear at excitation energies above 1.6 MeV. All the states, apart from the 1^-_2 and 0^+_1 and 1^+_1 are well separated in excitation energy by ~1 MeV. The separation between 1^-_2, the 0^+_1 and the 1^+_1 is of > 0.300 MeV. Only the 1^+_2 is expected to be unbound (S_n=2.82 MeV, S_{2n}=8.71 MeV).

Table 1: Spin and parity (1st column), theoretical excitation energies (2nd column) and shell model spectroscopic factors for ^{18}C and ^{18}N (3rd column), quantum numbers of the neutron coupled to the ^{18}C(0^+) and ^{18}N(0^+) core (4th column). In case that more than one component is significant, the SF is also shown in the 5th column. Only the states with large SF for the proton $1p_{1/2}$ and $1p_{3/2}$ states are shown.

d(^{19}N,^{3}He)^{18}C					
J^π	E_x (MeV)	SF(0+) WBT*	nlj		
0^+_1	0.0	0.90	$1p_{1/2}$		
2^+_4	6.43	0.50	$1p_{3/2}$		
2^+_5	8.09	0.96	$1p_{3/2}$		
1^+_4	9.90	0.44	$1p_{3/2}$		
2^+_{10}	10.80	0.26	$1p_{3/2}$		
d(^{19}N,^{3}H)^{18}N					
J^π	E_x (MeV)	SF(0+) WBT*	nlj	SF(0^+) WBT*	nlj
2^-_1	0.0	1.26	$1d_{5/2}$		
3^-_1	0.65	1.79	$1d_{5/2}$		
1^-_2	1.27	0.39	$2s_{1/2}$		
0^+_1	1.59	0.24	$1p_{1/2}$		
1^+_1	1.98	0.45	$1p_{1/2}$		
1^+_2	3.16	0.14	$1p_{3/2}$	0.27	$1p_{1/2}$

In summary, we intend to observe, for the first time, the proton single-particle states in ^{18}C, and measure their spectroscopic factors which carry relevant information on the Z=6 shell gap. This will be a unique opportunity to determine the microscopic origin of the spin-orbit splitting. In addition, cross-shell states in ^{18}N will help to refine nuclear structure calculations in the p-sd region.

2-Experimental method

2.1-Beam production

The ^{19}N secondary beam will be obtained via fragmentation in the LISE spectrometer from a primary beam of ^{22}Ne at 60 A. MeV. The primary beam will be slowed down in a production target of 2 mm thickness and in a degrader at the dispersive plane of 2.245 mm, made out of beryllium. The beam energy spread of the secondary beam DE/E will be controlled via the slits at the dispersive plane of the spectrometer. Keeping the moment slits F31 at $\pm$15 mm (Δp/p 1.8%), which corresponds to an energy dispersion of ΔE/E $\pm$ 2.5 % after the F62 slits, we will obtain a final secondary beam intensity of approximately 10^4 pps/eμA. Assuming a stable functioning of the cyclotrons, the primary beam could easily reach 8 eμA, resulting in a secondary beam intensity of 8 x10^4 pps. Information on the beam spot size will be obtained from ACTAR TPC. Normalisation of the secondary beam intensity will be achieved by using a fast counter just in front of the entrance window of ACTAR TPC, with exactly the same diameter. This device was successfully used in two experiments earlier 2019.

The estimated final secondary beam energy at the achromatic plane is 35 AMeV. The beam is expected to be pure since the Tz=+5/2 contaminants ^{21}O and ^{17}C are far away in F43. Timing between D4 and D6 will be measured with two fast counter detectors.

2.2 Experimental set-up

The experiment will be performed with the ACTAR TPC detector based on the active-target concept [Rog18]. This device allows to use a relatively thick target gas without loss of resolution. For our experiment, ACTAR TPC will be filled in with a mixture of D_2 (95%) + iC_4H_{10}(5%) gaz at approximately 1 bar and will be equiped with a first layer of DSSD Silicon detectors 1mm thick and a second layer of CsI detectors of 1.0 cm at forward angles. The first layer of DSSD Silicon detectors has a pitch size of 3.0 mm.

2.3-Kinematics and Cross sections

In this experiment we intend to identify isotopically both outgoing particles and to measure the energy and angle of the light ejectile and the beam-like fragment in order to have access to the full kinematics of the reaction. The unique capabilities of ACTAR TPC offer the possibility of reconstructing the reaction in 3 dimensions with high precision. Firstly, both particles will be seen at the same time in the pad-plane of the detector as their deposited energy is very similar, allowing to reduce significantly the uncertainty in the outgoing angles. This is very important, namely in the region where the kinematics bends. Secondly, isotopic identification of the heavy-like and ejectile-like particles will allow us to determine unambiguously the decay channel. In the case of the d(^{19}N,^{3}He)^{18}C, most of the expected states are above the S_n and S_{2n} separation energies, therefore distinguishing between ^{16}C , ^{17}C or ^{18}C will provide additional information on the structure of those states. Finally, the study of correlations between the heavy and light fragment will also be possible with this set-up.

Table 2 shows the range, deposited energy, angular straggling, energy straggling and the average ionization of the different particles involved in the reaction for the energies of interest (see kinematics in Fig. 1) in ACTAR TPC filled in with D_2 gaz at 1bar. Light ejectiles will be stopped in the first Si layer (see Table 2), therefore Particle IDentification (PID) will be performed using the energy loss in the pad plane and the total energy left in the Silicon wall. Previous measurements [RogT09,Mau18] have shown that the energy resolution measured in the pad plane is enough to distinguish H-like from He-like ejectiles and to identify them. Heavy fragments will stop in the CsI detectors (see Table 2) and will be identified using the energy deposited in the Silicons wall against the total energy measured in the CsI. A similar procedure was used previously in the following references [RogT09,Rog09] and gave successful results. Concerning the total kinematic energies, TKE, the one from the light particle will be obtained from the Silicons with an energy resolution of ΔE_{tot}^{Si} (FWHM)= 0.120 MeV and the one from the heavy particle will be measured in the CsI with an energy resolution of ΔE_{tot}^{CsI} (FWHM)= 0.300 MeV

Figure 1 : Kinematics for the light ejectilel of the reactions d(^{19}N,^{3}He)^{18}C, and d(^{19}N,t)^{18}N induced by ^{19}N at 35 AMeV

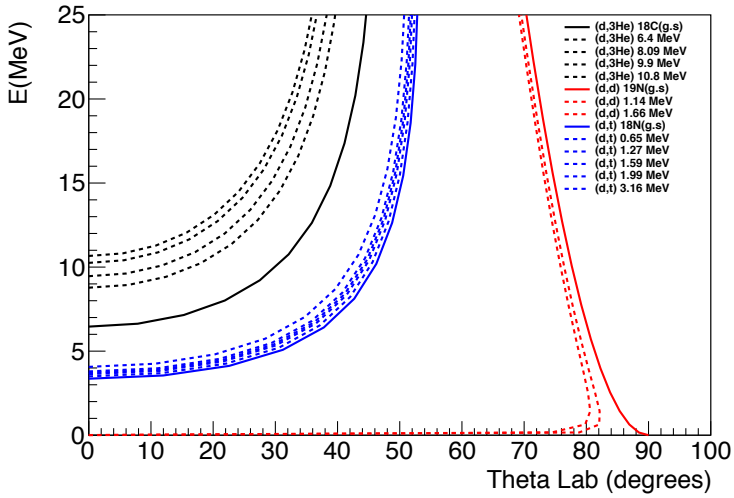

This is an ideal case for ACTAR TPC since the light and the heavy fragments have the same dynamic range and deposite similar amount of energy in the gaz. In addition, both particles have an average ionization energy within the gaz that is well above the threshold of ACTAR TPC set to 1 keV/mm [Mau18, Mau19]. This will allow us to see both tracks within the gaz and to determine the vertex of the reaction with very good resolution.

Particle	TKE (MeV)	R (mm)	ΔE (MeV)	$\sigma_{\theta strag}$ (degrees)	σ_{Estrag} (MeV)	<Ioniz> (keV/mm)
^{3}He	7	344	5.1	0.85	0.082	17
^{3}He	10	700	2.9	0.57	0.045	10
^{3}He	16	1485	1.9	0.34	0.042	6
^{18}C	540	24249	3.6	0.03	0.141	12
^{18}C	612	30595	3.3	0.03	0.141	11
^{18}C	648	33982	3.1	0.03	0.142	10
^{3}H	3.0	316	2.7	0.99	0.059	9
^{3}H	5.5	895	1.1	0.52	0.022	4
^{3}H	14	4692	0.5	0.19	0.020	1.6
^{18}N	504	15789	5.2	0.04	0.141	17
^{18}N	630	23762	4.3	0.03	0.142	14
^{18}N	666	26762	4.2	0.03	0.142	14

Table 2 : Particles involved in the reaction (1st column), total kinetic energy in MeV (2nd column), range (3rd column), deposited energy in MeV (4th column), sigma of the angular straggling (5th column), sigma of the energy straggling (6th column) and the average ionization of the particles (7th column) in the reaction in ACTAR TPC filled in with D_2 gaz at 1bar

Angular coverage depends on the vertex of the reaction, the dimensions of the Silicons (20 x 20 cm) encompasses angles in the laboratory between 0 and 45 degrees, corresponding to 0-25 in θ_{CM} for the (d,^{3}He) and to 0-15 in θ_{CM} for the (d,t) reaction. The highest cross section for the (d,^{3}He) and (d,t) reactions corresponds to the ^{3}He and ^{3}H particles emitted at forward center of mass angles between 0 and 15 degrees in the CM (see Figure 2). corresponding to θ_{lab} from 0 to 35 and 43 degrees, respectively.The resolution in excitation energy corresponding to this angular range is expected to be dominated by the uncertainty on the energy spread of the beam (ΔE (FWHM) = 33 MeV), angular resolution (Δθ(FWHM)<0.5 degrees) and energy resolution of the Silicon detectors (ΔE_{tot} (FWHM)= 0.120 MeV). The final value is determined to be ΔE_x (FWHM)=350 keV. This is enough to resolve the states in d(^{19}N,^{3}He)^{18}C where all

the states are well separated. It is important to note that the states are predicted to be unbound and therefore the resolution in excitation energy of the state will be mainly dominated by the width of the resonance. The case d(^{19}N,t)^{18}N is more challenging since the 1^-_2, and the 0^+_1 are 320 keV appart in excitation energy, and therefore there will be some overlap. However, those states have different orbital angular momentum and could be distinguish in the region between 5-10 θ_{CM} where the contribution from the l=0 removal is negligeable. For the 0^+_1 and the 1^+_1 states the expected separation is ~400 keV so just above the estimated energy resolution.

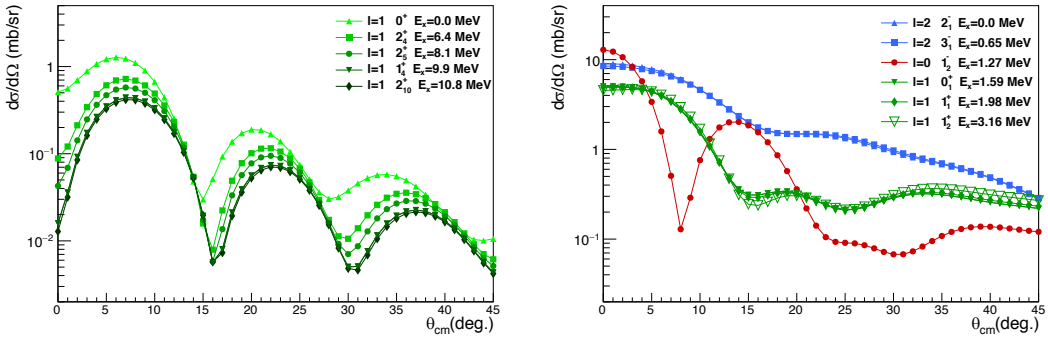

Figure 2: Theoretical differential cross section for the states of interest. Left : d(^{19}N,^{3}He)^{18}C, Right : d(^{19}N,t)^{18}N

3. Counting rates and beam time request

The requested beam time will be mainly determined by the cross section of the d(^{19}N,^{3}He)^{18}C reaction. The expected cross sections are shown in Fig. 2 for SF=1. Assuming an average value of $d\sigma/d\Omega$ ~ 0.01 mb/sr (taking into account the range of spectroscopic factors shown in Table 1) a target thickness of 3 x 10^{21} deuterons/cm^2 and a beam intensity of ^{19}N of 8 x 10^4 pps, we can get of the order of ~1400 particles in each state during 6 days of full beam time. This counting time would allow for reasonable measurements of the angular distributions of all the states. In addition, we request 2UT's days for secondary beam tuning and 2UT's more for in-beam calibrations with ACTAR-TPC

In summary we request a total of 22 UT's, 18 UT's for the data-taking, 2 UT's for the beam tunning and 2UT's for in-beam calibrations.

Bibliography

[Goe49] M. Goeppert Mayer, Phys. Rev. 75, 1969–1970 (1949); H.O. Jensen, ibid 75, 1766 (1949).

[Goe63] M. Goeppert Mayer, Nobel Lectures, Physics, 20–37 (1963).

[Pie93] S. C. Pieper and V. R. Pandharipande, Phys. Rev. Lett. 70, 2541–2544 (1993).

[Ong18] D. T. Tran, H. J. Ong et al., Nature communications 9 (2018) 1594

[Sta08] M. Stanoiu et al., Phys. Rev. C 78, 034315 (2008)

[Gau06] L. Gaudefroy et al., Phys. Rev. Lett 97, 092501 (2006)

[Bur14] G. Burunder et al., Phys. Rev. Lett 112, 042502 (2014)

[Ajz91] F. Ajzenberg-selove. Nucl. Physics A523,1 (1991)

[Ima04] N. Imai et al., Phys. Rev. Lett. 92, 062501 (2004).

[Wie08] M. Wiedeking et al., Phys. Rev. Lett. 100, 152501 (2008).

[Ong08] H.J. Ong et al., Phys. Rev. C 78, 014308 (2008).

[Pet12] M. Petri et al., Phys. Rev. C 86, 044329 (2012).

[Vos12] P. Voss et al., Phys. Rev. C 86, 011303(R) (2012).

[Ong18] D. T. Tran, H. J. Ong et al., Nature communications 9 (2018) 1594

[Kond09] Y. Kondo et al., Phys. Rev. C 79, 014602 (2009)

[AldT18] A. Revel et al., Phys. Rev. Lett. 120, 152504 (2018)

[AldT18] A. Revel Ph.D. Thesis https://tel.archives-ouvertes.fr/tel-02082089/document

[Wbt92] E. K. Warburton, B. A. Brown Phys. Rev. C 49, 923 (1993)

[Kim18] AIP Conference Proceedings 1947, 020006 (2018)

[Rog18] T. Roger et al., Nucl. Instrum. and Meth. A895 (2018) 126-134.

[RogT09]T. Roger Ph.D. Thesis 2009 http://theses.fr/2009CAEN2030

[Rog09] T. Roger et al., Phys. Rev. C 79, 031603 (R) (2009).

[Mau18] B. Mauss et al., EPJ Web. Conf. 174 (2018) 01010.

[Mau19] B. Mauss et al., « Commissioning of the ACtive TARget and Time Projection Chamber (ACTAR TPC)" Submitted to NIMA